

Pair supersolid of the extended Bose-Hubbard model with atom-pair hopping on the triangular Lattice

Wanzhou Zhang,^{1,*} Yancheng Wang,^{2,†} and Wenan Guo^{2,3,‡}

¹*College of Physics and Optoelectronics, Taiyuan University of Technology Shanxi 030024, China*

²*Physics Department, Beijing Normal University, Beijing 100875, China*

³*Kavli Institute for Theoretical Physics China, CAS, Beijing 100190, China*

(Dated: September 3, 2012)

We systematically study an extended Bose-Hubbard model with atom hopping and atom-pair hopping in the presence of a three-body constraint on the triangular lattice. By means of large-scale Quantum Monte Carlo simulations, the ground-state phase diagram are studied. We find a continuous transition between the atomic superfluid phase and the pair superfluid when the ratio of the atomic hopping and the atom-pair hopping is adapted. We then focus on the interplay among the atom-pair hopping, the on-site repulsion and the nearest-neighbor repulsion. With on-site repulsion present, we observe first order transitions between the Mott Insulators and pair superfluid driven by the pair hopping. With the nearest-neighbor repulsion turning on, three typical solid phases with $2/3$, 1 and $4/3$ -filling emerge at small atom-pair hopping region. A stable pair supersolid phase is found at small on-site repulsion. This is due to the three-body constraint and the pair hopping, which essentially make the model a quasi hardcore boson system. Thus the pair supersolid state emerges basing on the order-by-disorder mechanism, by which hardcore bosons avoid classical frustration on the triangular lattice. The transition between the pair supersolid and the pair superfluid is first order, except for the particle-hole symmetric point. We compare the results with those obtained by means of mean-field analysis.

PACS numbers: 75.10.Jm, 05.30.Jp, 03.75.Lm, 37.10.Jk

I. INTRODUCTION

The development in experimentally manipulating ultra-cold atoms in an optical lattice paved the way to simulate strongly interacting systems in condensed-matter physics¹. It provides very clean and tunable systems to study quantum phase transitions and exotic quantum states, e.g., superfluid, Mott insulator, which are not easily accessible in condensed matters. The condensation of paired electrons, which provides the basis of superconductivity of metallic superconductor, plays an essential role in modern condensed-matter physics. Thus realizing pairing related novel quantum states in the context of ultra-cold atoms has attracted considerable recent interest, both in theoretical and experimental research.

One candidate to achieve such states is lattice bosons with attractive on-site interactions, which is stabilized by a three-body constraint^{2,3}. The three-body constraint has been realized by large three-body loss processes^{4,5}. The system can be mapped into spin-one atoms at unit filling⁶. Besides the conventional single atom superfluid (ASF) state, a pair (dimer) superfluid (PSF) phase consisting of the condensation of boson pairs emerges under sufficiently strong attraction^{2,3}. The PSF state is manifested as a second-order effect in the atom hopping in the optical lattice. Various phase transitions among the atomic superfluid (ASF), Mott insulator (MI) and PSF are investigated in great detail^{2,3,7-11}. Both the ground state and the thermal phase diagrams are obtained. Although the pair supersolid (PSS) state was predicted in system with correlated hopping^{12,13} and the paired two-species bosons supersolid was predicted on the square

lattice¹⁴ with the attractive interaction between different species and the repulsion between the same species of atoms turning on, the pair (single species) supersolid was not found in the present system when the nearest-neighbor repulsion is included, except for an isolated continuous supersolid at the Dirac point². The reason might be the same instability of the supersolid state (SS) on the square lattice, on which the former research focused, for hardcore bosons^{15,16}.

Another practical way to access pairing phenomena is considering repulsive bound-atom pairs in optical lattice, which have been realized in experiments^{17,18}. The system can be reasonably described by explicitly including atom-pair hopping^{19,20} in the ordinary extended Bose-Hubbard model (EBH). Such a pair hopping can also be introduced in atom-molecule coupling system on the state-dependent optical lattice²¹, or by a mechanism based on transport-inducing collisions²². The resulted Bose-Hubbard Hamiltonian is thus

$$H = - \sum_i \mu n_i + \frac{U}{2} \sum_i n_i(n_i - 1) + \sum_{\langle i,j \rangle} V n_i n_j - t \sum_{\langle i,j \rangle} (a_i^\dagger a_j + a_i a_j^\dagger) - t_p \sum_{\langle i,j \rangle} (a_i^{\dagger 2} a_j^2 + a_i^2 a_j^{\dagger 2}), \quad (1)$$

where a_i^\dagger (a_i) creates (annihilates) a boson at site i , t is the atom hopping amplitude for nearest neighbor sites $\langle ij \rangle$, t_p is the pair-hopping amplitude, V the nearest-neighbor repulsion, μ the chemical potential, $U > 0$ the on-site repulsion. The three-body constraint is applied which requires the occupation number $n_i = 0, 1$, or 2 . It is naturally expected that PSF, MI and solid phases

should emerge at certain parameters.

The three-body constraint and the pair hopping makes the system resemble hardcore bosons. For hardcore bosons supersolid state emerges on the triangular lattice basing on an order-by-disorder mechanism, by which a quantum system avoids classical frustration^{23,24}. Aiming to realize PSS state, we thus focus on the triangular lattice. A preliminary mean-field (MF) analysis²⁵ does predict the PSS phase in such a system. In present work we systematically study the model by means of a large scale Quantum Monte Carlo simulation. The phase diagram of the system is studied in great detail. With the nearest-neighbor interaction turning on, we report three types of solid phases at small hopping strength. Increasing pair hopping t_p , we find the expected PSS phase.

This paper is organized as follows: We first discuss the ground state at the classical limit in Sec. II, which is useful to identify various solids and MI states, in which we are interested. We describe the quantum Monte Carlo (QMC) method and useful observables in Sec. III. We then present, in Sec. IV, QMC simulation results, comparing with the mean-field analysis. The results for the noninteracting ($U = V = 0$) case are described in Sec. IV A. Those for the interacting case $U \neq 0$, $V = 0$ are given in Sec. IV B and for the case $V \neq 0$ in Sec. IV C, focusing on the parameter regions where the pair supersolid phase emerges. The nature of related phase transitions are discussed. We conclude in Sec. V with discussions.

II. CLASSICAL LIMIT

We first study the zero temperature phase diagram in the classical limit ($t = 0$, $t_p = 0$) in the presence of the three-body constraint.

At half filling, the solid order is frustrated on the triangular lattice, and the classical model has a hugely degenerate ground state with an extensive zero-temperature entropy²⁶. We focus on the solid ordering, away from half filling, with wave vector $\mathbf{Q} = (4\pi/3, 0)$. The lattice is divided into three sublattices: A, B, C . The solid order is thus denoted as (n_A, n_B, n_C) or its equivalent permutations, where the numbers are the boson occupations on three sublattices, respectively. The energy per site is

$$e = -\mu \frac{n_A + n_B + n_C}{3} + V(n_A n_B + n_A n_C + n_B n_C) + U \frac{n_A(n_A - 1) + n_B(n_B - 1) + n_C(n_C - 1)}{6}. \quad (2)$$

By comparing energy per site, we obtain phase boundaries between various phases, as shown in Fig. 1. Three atom-pair solid phases appearing in the region $0 < U/V < 3$ are of special interest, which have two bosons sitting on one or two sublattices, as shown in Fig. 1(b), (c) and (d). They are denoted as SI, SII and SIII, with densities $\rho = 2/3, 1, 4/3$, respectively. Other solid states related with configurations $(0, 0, 1)$, $(1, 1, 0)$, $(1, 1, 2)$,

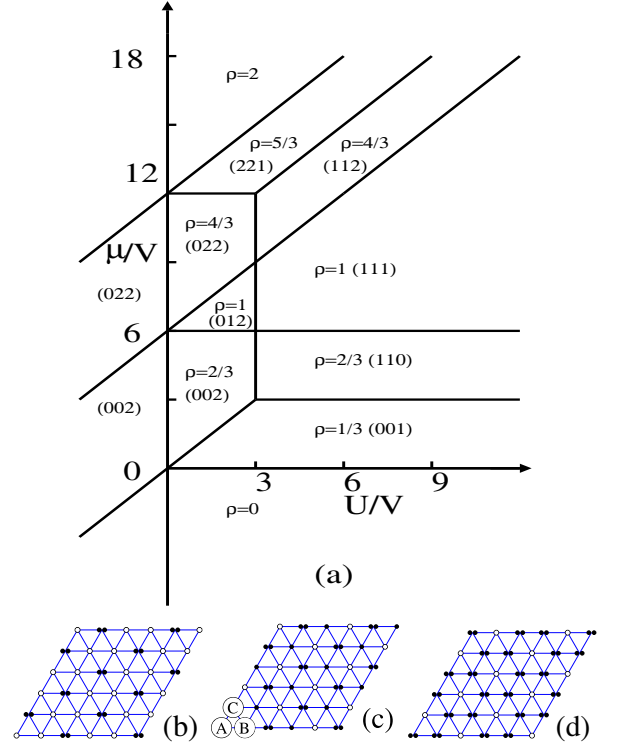


FIG. 1. (Color online) (a) The ground-state ($U/V - \mu/V$) phase diagram in the classical limit $t = 0$, $t_p = 0$. (n_A, n_B, n_C) denotes a solid order in a $\sqrt{3} \times \sqrt{3}$ ordering with wave vector $\mathbf{Q} = (4\pi/3, 0)$, where the numbers are boson occupations on three sublattices, respectively. (b) SI phase $(0, 0, 2)$ with filling $\rho = 2/3$. (c) SII phase $(0, 1, 2)$ with filling $\rho = 1$. (d) SIII phase $(0, 2, 2)$ with filling $\rho = 4/3$.

$(1, 2, 2)$ and MI states $(1, 1, 1)$ and $(2, 2, 2)$ are also found.

III. METHOD AND OBSERVABLES

We simulate the model (1) using the stochastic series expansion (SSE) QMC method²⁷ with the directed loop update²⁸, which is improved for the pair hopping. The head of a directed loop carries a create (annihilate) operator $a(a^\dagger)$ in the conventional directed loop algorithm for the BH model with single particle hopping. We improve the algorithm by allowing the head of a directed loop carry a pair create (annihilate) operators $a^{\dagger 2}(a^2)$ for the present EBH model with additional pair hopping terms. Similar improvement has been described in the literature²⁹. In the simulations, temperature is chosen as $\beta = L$ to ensure the system sitting in its ground state.

To distinguish the ASF and the PSF states, we define an even (odd) superfluid stiffness $\rho_s^{(\alpha)}$ as the order parameter³⁰:

$$\rho_s^{(\alpha)} = \frac{\langle W(\alpha)^2 \rangle}{4\beta(4t_p + t)}, \quad (3)$$

where β is the inverse temperature, α can be ‘even’ or ‘odd’; $W(\alpha)$ is the total even (odd) winding number. The factor ‘4’ multiplying t_p is due to the hopping of paired atoms³¹. The total superfluid stiffness is $\rho_s \equiv \rho_s^{(even)} + \rho_s^{(odd)}$. For a PSF state, we define the pair superfluid order parameter $\rho_s^{(p)} \equiv \rho_s^{(even)} - \rho_s^{(odd)} > 0$, while for an ASF state, $\rho_s^{(p)} = 0$, but $\rho_s \neq 0$. It is worthy to note that, without single atom hopping, $\rho_s^{(odd)}$ is guaranteed to be zero.

The structure factor is defined to characterize the solid order:

$$S(\mathbf{Q})/N = \langle \rho_{\mathbf{Q}} \rho_{\mathbf{Q}}^\dagger \rangle, \quad (4)$$

where $\rho_{\mathbf{Q}} = (1/N) \sum_i n_i \exp(i\mathbf{Q}\mathbf{r}_i)$. The solid states SI, SII and SIII share the same ordering at the wave vector $\mathbf{Q} = (4\pi/3, 0)$, but bear different values 4/9, 1/3, 4/9, respectively, in the perfect ordering.

IV. RESULTS

A. Non-interaction case: $U = 0, V = 0$; Competition between ASF and PSF

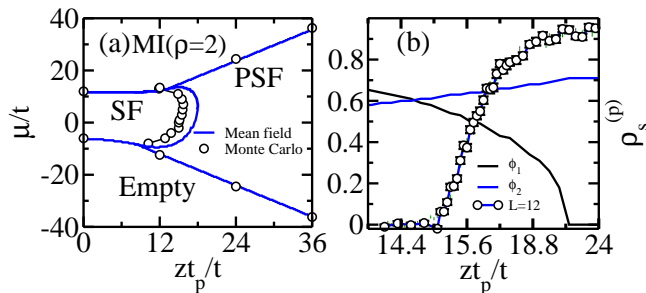


FIG. 2. (Color online) (a) $(zt_p/t, \mu/t)$ phase diagram of model (1) obtained by means of the MF (solid blue lines) and the QMC (circles) method, which contains Empty, MI, SF, and PSF phases at $U = 0, V = 0$. (b) Pair superfluid order parameter $\rho_s^{(p)}$ as a function of zt_p/t for $\mu = 0$ ($L = 12$). The MF order parameters ϕ_1 and ϕ_2 are also shown.

The ASF-PSF transition for model (1) without on-site repulsion U and nearest-neighbor repulsion V was previously discussed by means of MF analysis²⁵. Here we present our QMC results for such a system. To demonstrate the differences between our results and the MF results, we show both of them in Fig. 2. We find an Empty phase and a $\rho = 2$ MI phase at negative and large chemical potentials, respectively. The presence of the MI state is due to the three-body constraint. Between the Empty phase and the MI phase, there are two SF phases: an ASF phase and a PSF phase.

With small pair hopping $t_p \approx 0$, the system exhibits an Empty-ASF transition at $\mu = -6t$ and a SF-MI transition at $\mu = 12t$. This can be understood in the single

particle picture: to put a boson on the empty lattice gains potential energy $-\mu$ and kinetic energy $-zt$, where $z = 6$ is the coordination number of the triangular lattice. Adding a hole to the MI ($\rho = 2$) state costs chemical energy μ , while obtain kinetic energy $-2zt$. At large pair hopping $t_p \gg t$, the system shows a PSF-Empty transition at $\mu/t = -6t_p/t$. A pair of bosons emerging on the Empty phase gets $-2zt_p$ kinetic energy and potential energy -2μ . Similarly, the PSF-MI transition line is at $\mu/t = 6t_p/t$ by analyzing the emerging of a pair of holes on the MI state.

To demonstrate the transition between the ASF and the PSF states in more detail, we show here the system behaviors along $\mu = 0$ in Fig. 2(b). The PSF state was predicted at $t_p/t > 2.9$ in the MF frame using the criterion $\phi_1 \equiv \langle a \rangle = 0$ but $\phi_2 \equiv \langle a^2 \rangle \neq 0$ ²⁵. This transition is confirmed by our unbiased QMC simulations. However, the transition point is $t_p/t = 2.5$. The PSF state is characterized by $\rho_s^{(p)} > 0$. The phase transition between ASF and PSF is continuous. In the presence of strong on-site attractive interactions ($U < 0$), the PSF has been predicted in the lattice bosons with a three-body hard-core constraint^{8,9}. However, the transition between ASF and PSF phases is claimed to be first order⁸.

B. MI-PSF phase transitions for $U > 0$ and $V = 0$

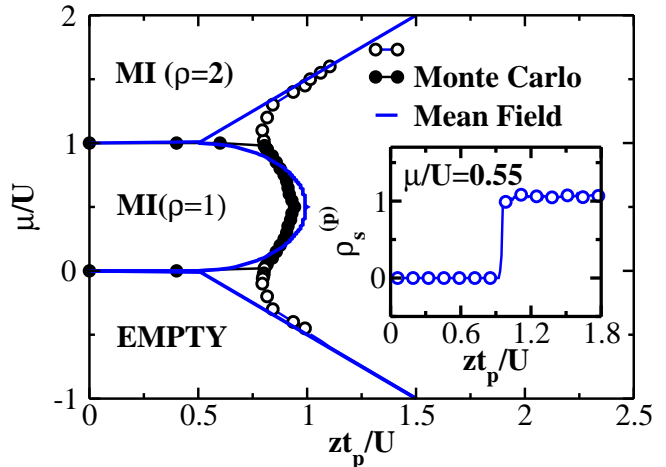


FIG. 3. (Color online) $(zt_p/U, \mu/U)$ phase diagram obtained by QMC (circles) and MF analysis (solid blue lines) at $t = 0, V = 0$, which contains the Empty, MI ($\rho = 1$), MI ($\rho = 2$), and PSF phases at $\mu/V = 0.55$. Open and solid circles correspond to continuous and first order transitions, respectively. The pair superfluid order parameter $\rho_s^{(p)}$ vs. zt_p/U is shown in the inset.

In the presence of the on-site repulsion U and the absence of the single atom hopping t , the ASF state disappears, instead an MI ($\rho = 1$) phase emerges. Without

three-body constraint, the general picture of the phase diagram has been studied by Zhou *et al* using the MF method²¹. We show here the phase diagram, under three-body constraint, obtained by using the MF method²⁵ and by the QMC simulations in Fig. 3. The phase boundaries obtained by using the two methods are in good agreement for large t_p . The Empty-PSF phase transition line is straight with the slope $\mu/(zt_p) = -1$, which can be understood in the single particle picture: A boson pair emerging in the empty phase gets $-2zt_p$ kinetics energy and -2μ potential energy. Similarly, the MI($\rho = 2$)-PSF boundary is also straight with a slope $\mu/(zt_p) = 1$ at large t_p . QMC simulations provide more accurate boundaries between the MI phases and PSF phase. The $\rho = 2$ MI-PSF transition is found to be continuous and the MI($\rho = 1$)-PSF transition is first order, as illustrated in the inset of Fig. 3.

C. Pair supersolid phase for $U = 0$ and $U > 0$

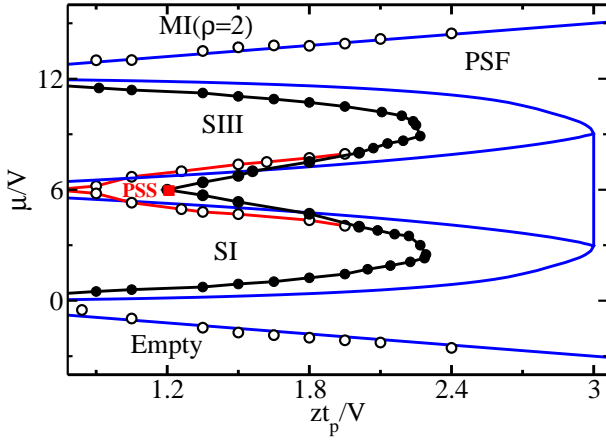


FIG. 4. (Color online) $(zt_p/V, \mu/V)$ phase diagram obtained by QMC (circles) and the MF analysis (solid blue lines) of model (1) at $t = 0, U = 0$, which contains the Empty, MI, SI, SIII, PSF and PSS phases. Open and solid circles correspond to continuous and first order transitions, respectively. The PSS-PSF transition is first order except for the $\mu/V = 6$ point marked by a red square³².

As a result of the absence of on-site repulsion, boson pairs easily emerge on a site without costing of any potential energy. In the limit $t_p/t \rightarrow \infty$ (or $t = 0$), boson pairs (hole pairs) can easily hop on the lattice, forming a PSF phase. When the nearest-neighbor interaction V present, solid ordering appears naturally. Hardcore bosons with single-atom hopping on the triangular lattice has an SS phase between two solid phases $((0, 0, 1)$ and $(0, 1, 1))$ ^{23,24}. Bosons on the triangular lattice with pair hopping under three-body constraint mimic such behavior with the two solid phases replaced by the $(0, 0, 2)$ and $(0, 2, 2)$ solid phases respectively. The global phase diagram obtained by means of the MF method²⁵

and QMC simulations is shown in Fig 4. Both method predict a PSS phase between the two solid phases. However, the PSS region is much smaller in the QMC phase diagram. This is due to quantum fluctuations ignored in the MF analysis.

We further illustrate the phase diagram along two lines: one is $zt_p/V = 1.05$, the other is $\mu/V = 7.5$.

Figure 5 shows the density ρ , structure factor $S(\mathbf{Q})/N$ and pair superfluid order parameter $\rho_s^{(p)}$ as functions of μ/V along the $zt_p/V = 1.05$ line. Considering the hole-particle symmetry, we only present results for $\mu/V \leq 6$. The PSS state emerges clearly between the two solid phases (SI and SIII), which is further proved by a finite-size scaling analysis of the structural factor and the pair superfluid stiffness $\rho_s^{(p)}$ (not shown).

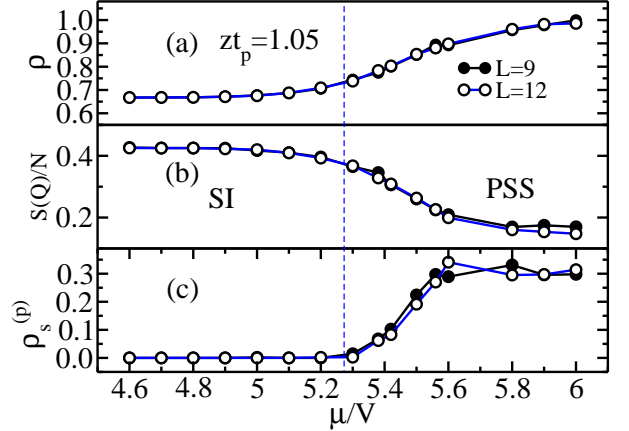


FIG. 5. (Color online) The density ρ , structural factor $S(\mathbf{Q})/N$, PSF stiffness $\rho_s^{(p)}$ as functions of μ/V at $zt_p = 1.05$.

Next, we scan the pair hopping t_p along $\mu/V = 7.5$. The density ρ , structural factor $S(\mathbf{Q})/N$ and pair superfluid order parameter $\rho_s^{(p)}$ as functions of the pair hopping t_p are shown in Fig. 6(a), with the PSS state emerging in the region $1.668 < zt_p/V < 1.788$. Figure 6(b) shows a finite size scaling analysis of the pair superfluid order parameter $\rho_s^{(p)}$ and the structural factor $S(\mathbf{Q})/N$ at $zt_p/V = 1.74$, $\mu/V = 7.5$, which proves that the state is indeed a pair supersolid.

The phase transition between the PSS and other states are interesting. The PSS-SI(SIII) transition is continuous from continuous variation of the density and the structure factor, while the PSS-PSF transition is first order, except for the particle-hole symmetric point³², as illustrated by the jump of the structural factor and the PSF order parameter in Fig. 6(a). From the jumps of the PSF order parameter and the structural factor (not shown), the PSF-solid phase transitions are also first order.

We now check whether the pair supersolid phase could survive as a weak on-site repulsion turns on. Figure 7 shows the MF and QMC phase diagram at weak repul-

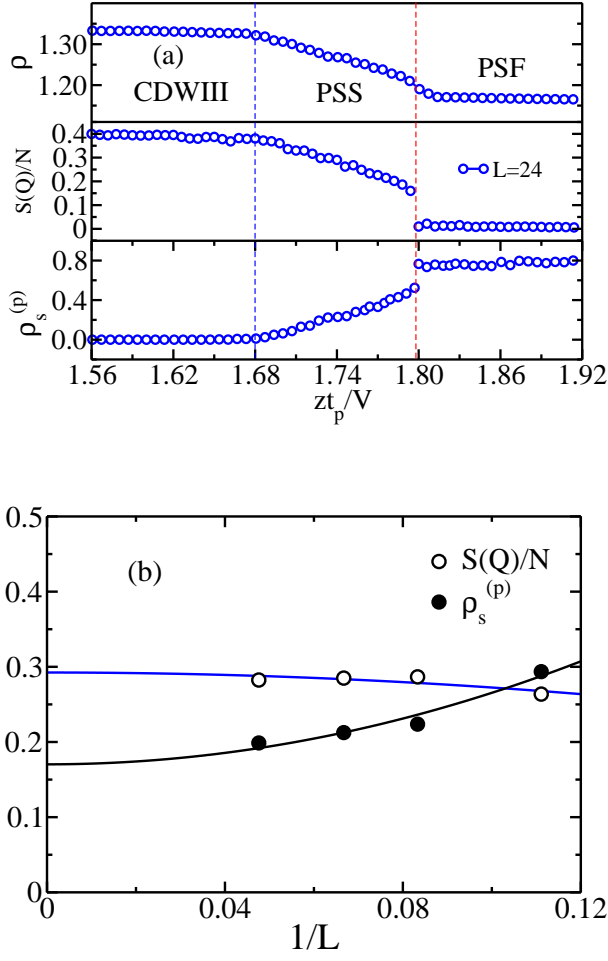


FIG. 6. (Color online) (a) The density ρ , structural factor $S(\mathbf{Q})/N$, and PSF order parameter $\rho_s^{(p)}$ as functions of pair hopping zt_p/V at $\mu/V = 7.5$. (b) Finite size scalings of the structural factor $S(\mathbf{Q})/N$ and PSF order parameter $\rho_s^{(p)}$ at $zt_p/V = 1.74$ and $\mu/V = 7.5$, showing PSS character at thermodynamic limit.

sion $U/V = 1$. Three new solid phases, i.e., SII, $(0, 0, 1)$ and $(2, 2, 1)$, emerge comparing to the case $U = 0$. The PSS phase persists. Increasing t_p , all solid phases melt into the PSF phase eventually. The persistence of the PSS state at weak on-site repulsion is because that the PSS state depends strongly on the frustrated geometrical structure of the triangular lattice for hardcore bosons: although the maximum occupation is two, the pair hopping essentially make the model (1) a quasi hardcore boson system. Weak on-site repulsions do not change this feature.

At the large U/V limit, the phase diagram should reduce to the one shown in Fig. 3. This suggests the PSS phase will disappear finally. Indeed, we don't find PSS phase when $U/V \geq 4$.

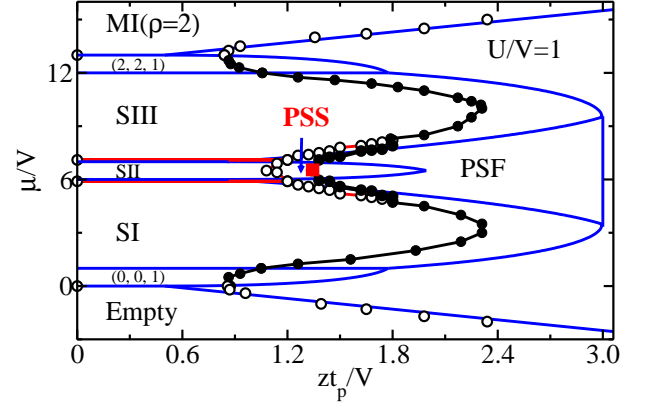


FIG. 7. (Color online) $(zt_p/V, \mu/V)$ phase diagram obtained by QMC (circles) and the MF (solid blue lines) method at $U/V = 1$, which contains the Empty, MI($\rho = 1, \rho = 2$), SI, SII, SIII, $(0, 0, 1)$, $(2, 2, 1)$, PSF and PSS phases. Open and solid circles correspond to continuous and first order transitions, respectively. The red square marks the special high symmetric point.

V. CONCLUSION

We have studied the ground-state phase diagram of the extended Bose-Hubbard model with explicit atom-pair hopping terms, under the three-body constraint, on the triangular lattice. Experimentally, the atom-pair hopping physics has been realized. The triangular optical lattice can also be implemented by three beams of lasers³³. The atom-molecule coupling system²¹ and the spin-1 boson system⁶ in state dependent optical triangular lattice are also candidates to simulate pair related quantum phenomena. By means of the improved SSE QMC method, we obtain accurate phase diagrams at various parameter values. Rich solid phases and the pair superfluid phase are found, as well as the pair supersolid phase, which emerges when the nearest-neighbor repulsion and the pair hopping are present, under the condition that the on-site repulsion is not large. The three-body constraint and the pair hopping essentially make the model (1) a quasi hardcore boson system. Weak on-site repulsions do not change this feature. Therefore, the mechanism of forming the PSS state is the same as that of forming SS state for hardcore bosons on the triangular lattice. The properties of phase transitions involved, e.g., the ASF-PSF, the MI-PSF, the PSS-PSF, the PSF-solid transitions, are studied.

It would be interesting to study the finite temperature properties of the present model. The three-body constraint due to the three-body loss⁴, can be suppressed, or even inhibited by the quantum Zeno effect³⁴. Thus the quantum Zeno effect provides us a basis to study the pair physics without three-body constraint.

ACKNOWLEDGMENTS

W.Z. thanks the Found from Taiyuan University of Technology, the NSF of Shanxi Province, and discussions

with Y.-B. Zhang and R.-X. Yin. The work is supported by the NSFC under Grant No.11175018.

-
- * zhangwanzhou@tyut.edu.cn
† wangyancheng@mail.bnu.edu.cn
‡ wagu@bnu.edu.cn
- ¹ I. Bloch, J. Dalibard, and W. Zwerger, *Rev. Mod. Phys.* **80**, 885 (2008); M. Lewenstein, A. Sanpera, V. Ahufiner, B. Damski, A. Sen, and U. Sen, *Adv. Phys.* **56**, 243 (2007).
 - ² S. Diehl, M. Baranov, A. J. Daley, and P. Zoller, *Phys. Rev. Lett.* **104**, 165301 (2010).
 - ³ S. Diehl, M. Baranov, A. J. Daley, and P. Zoller, *Phys. Rev. B* **82**, 064509 (2010); *Phys. Rev. B* **82**, 064510 (2010).
 - ⁴ A. J. Daley, J. M. Taylor, S. Diehl, M. Baranov, and P. Zoller, *Phys. Rev. Lett.* **102**, 040402 (2009).
 - ⁵ M. Roncaglia, M. Rizzi, and J. I. Cirac, *Phys. Rev. Lett.* **104**, 096803 (2010).
 - ⁶ L. Mazza, M. Rizzi, M. Lewenstein, and J. I. Cirac, *Phys. Rev. A* **82**, 043629 (2010).
 - ⁷ Y. W. Lee and M. F. Yang, *Phys. Rev. A* **81**, 061604 (2010).
 - ⁸ K. K. Ng and M. F. Yang, *Phys. Rev. B* **83**, 100511(2011).
 - ⁹ L. Bonnes and S. Wessel, *Phys. Rev. Lett.* **106**, 185302 (2011).
 - ¹⁰ Y. C. Chen, K. K. Ng, and M. F. Yang, *Phys. Rev. B* **84**, 092503 (2011).
 - ¹¹ L. Bonnes and S. Wessel, *Phys. Rev. B* **85**, 094513 (2012).
 - ¹² K. P. Schmidt, J. Dorier, A. Läuchli, and F. Mila, *Phys. Rev. B* **74**, 174508 (2006).
 - ¹³ H. C. Jiang, L. Fu, and C. K. Xu, *Phys. Rev. B* **86**, 045129(2012).
 - ¹⁴ C.-M. Chung, S. Fang, and P. Chen, *Phys. Rev. B* **85**, 214513 (2012).
 - ¹⁵ P. Sengupta, L. P. Pryadko, F. Alet, M. Troyer, and G. Schmid, *Phys. Rev. Lett.* **94**, 207202 (2005).
 - ¹⁶ G. G. Batrouni and R. T. Scalettar, *Phys. Rev. Lett.* **84**, 1599 (2000).
 - ¹⁷ S. Fölling, S. Trotzky, P. Cheinet, M. Feld, R. Saers, A. Widera, T. M. Ller, and I. Bloch, *Nature* **448**, 1029 (2007).
 - ¹⁸ K. Winkler, G. Thalhammer, F. Lang, R. Grimm, J. H. Denschlag, A. J. Daley, A. Kantian, H. P. Böchler and P. Zoller, *Nature* **441**, 853(2006).
 - ¹⁹ J. Q. Liang, J. L. Liu, W. D. Li, and Z. D. Li, *Phys. Rev. A* **79**, 033617 (2009).
 - ²⁰ Y. M. Wang and J. Q. Liang, *Phys. Rev. A* **81**, 045601 (2010).
 - ²¹ X. F. Zhou, Y. S. Zhang, and G. C. Guo, *Phys. Rev. A* **80**, 013605 (2009).
 - ²² Maria Eckholt and Juan José García-Ripol, *Phys. Rev. A* **77**, 063603(2008); *New Journal of Physics* **11**, 093028 (2009).
 - ²³ S. Wessel and M. Troyer, *Phys. Rev. Lett.* **95**, 127205 (2005).
 - ²⁴ M. Boninsegni and N. Prokof'ev, *Phys. Rev. Lett.* **95**, 237204 (2005).
 - ²⁵ Y.-C. Wang, W.-Z. Zhang, and W.-A. Guo, to be published.
 - ²⁶ G. H. Wannier, *Phys. Rev.* **79**, 357 (1950).
 - ²⁷ A. W. Sandvik, *Phys. Rev. B* **59**, R14157 (1999);
 - ²⁸ O. F. Syljuåsen and A. W. Sandvik, *Phys. Rev. E* **66**, 046701 (2002).
 - ²⁹ L. Pollet, M. Troyer, K. Van Houcke, and S. M. A. Rombouts, *Phys. Rev. Lett.* **96**, 190402 (2006); L. Pollet, Ph. D. thesis, Universiteit Gent, 2005.
 - ³⁰ E. L. Pollock and D. M. Ceperley, *Phys. Rev. B* **36**, 8343 (1987).
 - ³¹ A. W. Sandvik, *Phys. Rev. Lett.* **104**, 177201 (2010).
 - ³² Lars Bonnes and Stefan Wessel, *Phys. Rev. B* **84**, 054510 (2011).
 - ³³ C. Becker *et al.*, *New J. Phys.* **12** 065025(2010).
 - ³⁴ R. Schoöthold and G. Gnanapragasam, *Phys. Rev. A* **82**, 022120 (2010).